

1 **Flow structures over mesophotic coral ecosystems in the eastern Gulf of Mexico**

2

3 Arnoldo Valle-Levinson¹, Villy H. Kourafalou², Ryan H. Smith³, Yannis Androulidakis^{2,4}

4

5 ¹University of Florida, Civil and Coastal Engineering Department, arnoldo@ufl.edu

6 ²University of Miami, Rosenstiel School of Marine and Atmospheric Science,
7 vkourafalou@rsmas.miami.edu & iandroul@rsmas.miami.edu

8

9 ³NOAA Atlantic Oceanographic and Meteorological Laboratory, ryan.smith@noaa.gov

10

11 ⁴Norwegian Meteorological Institute, Bergen, 5007, Norway

12

13 Keywords: Pulley Ridge, Dry Tortugas, interconnectivity, Loop Current, Florida Current

14

15

16 **Abstract**

17 Simultaneous time series of current velocity profiles are used to characterize flow
18 structures over intermediate-depth coral ecosystems in the eastern Gulf of Mexico.
19 Understanding of temporal variability and spatial coherence in flow is necessary to establish
20 connectivity among these ecosystems. Time series were collected at Pulley Ridge (the
21 westernmost site), Northern Dry Tortugas, and Southern Dry Tortugas. Overlapping data
22 spanned the period from March 22, 2013 to June 20, 2015. The strongest currents were
23 approximately 1 m s^{-1} southeastward at Pulley Ridge. Subtidal velocities from the three sites
24 were decomposed into real-vector, concatenated empirical orthogonal functions (EOFs). Results
25 from EOFs indicated that Mode 1, which explained 63% of the subtidal variations, was roughly
26 in the same direction at each of the three sites. Mode 1 directionality indicated potential
27 interconnectivity between Pulley Ridge and Southern Dry Tortugas, and between Northern Dry
28 Tortugas and Pulley Ridge. Mode 1 also suggested limited to no connectivity between the two
29 Dry Tortugas sites as the flows over the two sites were parallel. Mode 2 explained close to 24%
30 of the variability and showed incoherence among the three sites. Wavelet analysis of EOF
31 coefficients indicated dominance of >1 week variability in this region. Flow variability may be
32 associated with wind forcing and Loop Current variability as confirmed by satellite altimetry.
33 Wind forcing caused part of the intra-monthly (<1 month) periodicity in flows. Sea level in the
34 area of the Loop Current, as derived from EOF application on altimetry data during the period of
35 velocity measurements, was related to Mode 1 of the currents at sub-monthly (>1 month) periods.
36 The relationship was more robust, but inverse, when comparing sea level off the northwestern
37 coast of Cuba to the Mode 1 of the currents. These results characterize physical connectivity
38 among South Florida coral ecosystems and have biophysical implications for coral fish
39 populations.

40 **1. Introduction**

41 Mesophotic coral reefs develop at intermediate light levels (30-100 m deep, Kahng et al.,
42 2010) and are also referred to as ‘twilight’ reef ecosystems (Brokovich et al., 2008). In contrast
43 to shallow water reefs, mesophotic reefs are typically insulated from the influence of wave action
44 (Lesser et al., 2009) and from high temperature stress (e.g. Hoegh-Guldberg et al., 2007). Still
45 unknown is the potential role of these mesophotic reefs in counteracting massive bleaching on
46 shallow water reefs. A crucial topic that should allow evaluating such role of mesophotic reefs
47 and manage their protection is understanding the connectivity of populations between healthy
48 and degraded ecosystems. Physical connectivity among reef sites can be established through the
49 study of regional current velocity structures. In the Gulf of Mexico, the regional circulation is
50 dominated by the Loop Current – Florida Current system, part of the Gulf Stream western
51 boundary current.

52 This study aims at providing basic information on flow structures at the Pulley Ridge and
53 Dry Tortugas regions, near the southern edge of the West Florida Shelf at the eastern Gulf of
54 Mexico. Its specific objective is to determine the influence on such flow structures of local wind
55 stresses and of regional circulation patterns, such as the Loop Current variability. This study
56 relies on a unique data set of currents from a mooring array at 3 sites in the study area. This is the
57 first time that long-term (almost 3 years) current velocity profiles have been collected at any
58 mesophotic reef, including the Pulley Ridge and Dry Tortugas. The dataset has already been used
59 to discuss physical and biophysical connectivity around the eastern Gulf of Mexico and the
60 Florida Keys (Kourafalou et al., 2018). The data validated numerical simulations that illustrated
61 the influence of the Loop Current - Florida Current system on local dynamics of the Pulley Ridge
62 and Dry Tortugas reefs. Withdrawal of the Loop Current - Florida Current system from the
63 continental shelf break may favor onshore flows that can carry open-sea waters over the coral

64 reefs. Simulations also showed that only the area over the Northern Dry Tortugas, located farther
65 from the shelf break (Fig. 1), was influenced by the wind. The formation of local cyclonic eddies
66 near the Dry Tortugas can also promote or hinder physical connectivity between these reefs
67 (Kourafalou et al., 2018). Biophysical simulations (Vaz et al., 2016), based on the same
68 hydrodynamic simulations as Kourafalou et al. (2018), indicated mesophotic-shallow
69 connections, with larvae spawned at Pulley Ridge reaching the Florida Keys settlement grounds.
70 The findings of these studies suggest that a combination of regional circulation, wind-induced
71 shelf circulation and eddies associated with the Loop Current – Florida Current system control
72 the connectivity between these mesophotic coral reefs and also impact the circulation at
73 shallower reefs downstream in the Florida Keys. Other factors related to wave shoaling, such as
74 wave-induced currents and wave breaking, might play a role on the local circulation regime (e.g.,
75 Sous et al. 2017). Wave-shoaling influence will be appreciable in coastal regions and narrow
76 passages between islands (e.g. Florida Keys). The study area is characterized by open and
77 relatively deep coral reef regions where wind waves remain deep.

78 Model findings (Kourafalou et al., 2018; Vaz et al., 2016) motivated further verification
79 of connectivity patterns through Empirical Orthogonal Function (EOF) analysis of the moored
80 observations. This analysis illustrated the dominant spatial structures displayed by the flow and
81 described how such spatial structures varied over time. The ultimate project goal is to use a
82 unique data set covering complex circulation patterns around mesophotic reef ecosystems to
83 understand the physical connectivity mechanisms, thus helping managers develop reliable
84 strategies to protect these economically relevant, but environmentally fragile, resources. In
85 addition, the results presented here provide unique information for the understanding of physical
86 connectivity in mesophotic reefs, in tropical and subtropical systems, and in the eastern Gulf of
87 Mexico in particular.

88

89 **2. Study Area**

90 The mesophotic reefs of the Pulley Ridge region, including Dry Tortugas, are located on
91 the continental shelf of the eastern Gulf of Mexico, west of Florida Keys, between 83°W and
92 84°W, and between 25.4°N and 25.75°N (Fig. 1). The reefs are near semicircular shoals between
93 1 and 15 km in diameter, and between 1 and 10 km from the shelf break, where the Loop Current
94 - Florida Current system evolves in the Straits of Florida. The reefs are scattered over a sloping
95 shelf that increases from 20 to 70 m depth over ~90 km.

96 The region is forced by tides, heat fluxes and momentum fluxes, including the Loop
97 Current - Florida Current system (Gordon, 1967; Johns et al., 2002) and mesoscale cyclonic
98 eddies (Sponaugle et al., 2005; Kourafalou and Kang, 2012; Kourafalou et al., 2018). At Pulley
99 Ridge, on the basis of nearly 3 years of measurements obtained in this study, the amplitude of the
100 O1 (33.4% of sea level variability) tidal constituent is 0.11 m while the K1 (31.3% of sea level
101 variability) is also 0.11 m. The amplitude for M2 (20.6% sea level variability) is 0.09 m and for
102 S2 (4.6% sea level variability) is 0.04 m. These 4 constituents explain close to 90% of the sea
103 level variability according to the data collected. Other relevant tidal harmonics, contributing >1%
104 of the water level variability, are P1, Q1 (both diurnal), SSA (semiannual), and SA (annual). The
105 ratio of diurnal to semidiurnal amplitudes is 1.7, which indicates a regime of mixed tides with
106 diurnal dominance. Maximum tidal ranges are typically 0.6 m but can reach 0.7 m when the
107 synodic (14.77 days) and declinational (13.66 days) fortnights coincide, while minimum ranges
108 are between 0.1 and 0.15 m. Despite its microtidal regime, tidal variations are prevalent in the
109 currents observed. The inertial period at the latitude of the study (24°N) is close to 30 h. The
110 study area represents a zone of confluence of the Loop Current -Florida Current system at the
111 shelf break with mixed tidal currents on the west Florida shelf.

112 Momentum fluxes are related to southward wind stress from October to March and
113 northward from April to September (e.g. Boicourt et al., 1998; Zavala-Hidalgo et al., 2014). Heat
114 fluxes follow the expected annual cycle of heat gain from April to September and heat loss from
115 October to March with perturbations from advective fluxes related to the Loop Current (Etter,
116 1983). Freshwater influence is appreciable in Florida Bay from May to October (Lee et al., 2006;
117 2008; Stabenau and Kotun, 2012) but remains shoreward from the Pulley Ridge region.
118 Additional forcing from the Loop Current -Florida Current system depends on incompletely
119 understood processes in the Yucatan channel (Weisberg and Liu, 2017). This current system can
120 provide physical connectivity between the Northern Gulf of Mexico and the Florida Keys
121 (Chang and Oey, 2013; Schiller and Kourafalou, 2014; Le Hénaff and Kourafalou, 2016;
122 Androulidakis et al., 2019), and between the Caribbean reefs and the Florida Keys (Sheinbaum et
123 al., 2002). The study area represents a zone of confluence of wind-driven currents and mixed
124 semidiurnal tidal currents on the shelf, and the Loop Current - Florida Current system at the shelf
125 break.

126

127 **3. Data collection and analysis**

128 **3.1 Data collection**

129 Three bottom-mounted Teledyne RD Instruments Workhorse acoustic Doppler current
130 profilers (ADCPs) were deployed at Pulley Ridge, Southern Dry Tortugas and Northern Dry
131 Tortugas (Fig. 1) concurrently for 27 months. Deployments sought to document the overall
132 temporal and spatial variability of flows at the mesophotic Florida reefs. The three ADCPs were
133 mounted on trawl-resistant frames. A 307.2 kHz ADCP was deployed at Pulley Ridge (24°
134 42.00380'N, 083° 40.46700'W) in a depth of 66.5 meters, and was the westernmost site. This
135 instrument recorded hourly ensembles of 70 pings with a vertical resolution (bin size) of 4 m

136 from August 16, 2012 to June 20, 2015. A 614.4 kHz ADCP was moored at a depth of 54.3 m at
137 Northern Dry Tortugas (24° 46.45050'N, 083° 05.66814'W) from August 15, 2012 to June 23,
138 2015. Profiles were recorded in ensembles of 120 pings every hour, also with a 4 m bin size. The
139 mooring at Southern Dry Tortugas (24° 28.54390'N, 083° 09.21180'W) had a 307.2 kHz ADCP
140 at a depth of 66.3 m. Velocity profiles were recorded hourly at 70 pings per ensemble, in 4-m
141 bins, between March 22, 2013 and June 24, 2015.

142 The ADCP locations were chosen to capture flow structures within the mesophotic coral
143 reef area of Southeast Florida. The site at Pulley Ridge was chosen within the Habitat Area of
144 Particular Concern, to avoid trawling and to minimize possible local bathymetric effects. The
145 Dry Tortugas sites were also chosen to reduce shadowing effects from nearby shoals (e.g.,
146 Riley's Hump to the south, Sherwood Forest to the north). Mooring locations had to be outside
147 of the Dry Tortugas preserve areas (if only by a few meters) to minimize permitting challenges.

148 Wind velocity data and Gulf of Mexico Loop Current position were used to try to explain
149 some of the variability observed in the current profiles at the 3 sites. Wind velocity data were
150 obtained from Vaca Key, Florida station (VCAF1; 24.711° N, 81.107° W) of the National Data
151 Buoy Center of the National Oceanic and Atmospheric Administration in the United States. It is
152 the closest station to the mooring sites with complete data sets. It is also representative of the
153 wind conditions over the southern Western Florida shelf as shown by wind comparisons between
154 different locations over the Pulley Ridge and Tortugas areas (Kourafalou et al., 2018;
155 Androulidakis et al., 2018). Wind speed and direction were obtained at hourly intervals that
156 overlapped the common observational period of the three moorings from March 2013 to July
157 2015.

158 Loop Current information was derived from satellite sea surface height anomalies
159 (SSHAs) every 5 days in the Gulf of Mexico on a grid with a spatial resolution of 1/6° (Zlotnicki

160 et al., 2016). Data were retrieved for the period March 2013 to August 2015. Five possible
161 indices were explored to represent the Loop Current. The first index was described with the
162 temporal variability (or coefficients) of the first three EOF of SSHA data, averaged over a
163 horizontal box. This box was selected on the Loop Current position in EOF Mode 1. The three
164 empirical modes, together, explained close to half of the variability of SSHAs (see Section 3.2).
165 The second and third indices for the Loop Current were derived from the average SSHA values
166 in a) the same box selected from the EOFs (second index), and b) a box NW of Cuba, where
167 EOF Mode 1 had a trough (third index). The fourth index was the same index used by
168 Kourafalou et al. (2018), based on the 17 cm sea surface height contour (Leben, 2005). The fifth
169 index was represented by daily values of the Florida Current transport. Values were obtained
170 from a submarine cable, between Florida and Bahamas at the northern Straits of Florida (see
171 Acknowledgments) and were filtered with a Lanczos filter centered at 30 days to eliminate intra-
172 monthly variations.

173

174 **3.2. Data Analysis**

175 Concatenated, real-vector EOFs (Kaihatu et al., 1998) were calculated for all station data
176 together, to describe the dominant vertical structure (or modes) of currents at the 3 sites and to
177 establish the temporal variability of the dominant modes. Estimates were made on the velocity
178 vectors $\vec{v}(z, t)$, where z is depth and t is time, after tidal and inertial variations were filtered with
179 a Lanczos window (e.g. Thomson and Emery, 2014) centered at 34 h. Velocity vectors \vec{v} were
180 concatenated with the two horizontal velocity components (u, v) at the 3 sites. The concatenated
181 matrix \mathbf{V} , with the velocity components of the 3 sites, had 70 rows associated with every u and v
182 times series. In essence, the EOF analysis consists of solving the eigenvalue problem associated
183 with the covariance matrix of \mathbf{V} . The eigenvectors obtained from the eigenvalue problem

184 represent the prevailing velocity profiles. The eigenvalues represent the variance explained by
185 each EOF Mode and the coefficients of the eigenvectors depict the temporal evolution of the
186 current profiles. The EOF analysis synthesized the data collected by the ADCPs and provided
187 information on the dominant structure of the velocity profiles, as well as their temporal
188 variability.

189 Continuous wavelet transforms (e.g., Torrence and Compo, 1998) converted the temporal
190 variability of EOF modes 1 and 2 of the flow into time-varying spectra, by using a 4th order
191 Morlet wavelet. Wavelet transforms represent here the changes over time of the dominant
192 periods of subinertial variability at each sampling site. Wavelet transforms for EOF Mode 1 of
193 subtidal currents were compared then to the transform of the Loop Current index and to the
194 transform of each component of the wind. The comparison was made through a normalized
195 cross-wavelet, or wavelet coherence. Wavelet coherence between pairs of variables allowed
196 determination of instances when flow variability was consistent with the Loop Current - Florida
197 Current system or with wind. Each of the analyses outlined above is presented next as performed
198 on the measured time series.

199

200 **4. Results**

201 This section presents the low-pass filtered velocity components to compare qualitatively
202 the variability at the 3 sites. Subsequent results obtained from the EOF analyses put such a
203 qualitative comparison into statistical context. The spatial structure of modes 1 and 2 is then
204 placed in the regional perspective. Nearly depth-independent flows represent these 2 modes,
205 which together explain 87% of the variability throughout the 27 months of measurements.
206 Ensuing portrayal of wavelet power spectra of the time series of current velocity EOF modes 1
207 and 2 illustrates instances of most energetic flow and their typical period of variability. EOF

208 Mode 1 of subtidal currents is then compared qualitatively to a Loop Current index and to the
209 wind velocity components. The qualitative relationships are then explored statistically with the
210 wavelet transform of EOF 1 being compared to that of the Loop Current index and of the wind
211 velocity components.

212

213 **4.1 Low-pass filtered velocities**

214 Flows at Pulley Ridge were predominantly southeastward (Fig. 2), consistent with the
215 direction of the Loop Current transport from the Gulf of Mexico toward the Florida Current
216 genesis. The zonal component of subtidal velocity at Pulley Ridge (PR in Fig. 2) was
217 predominantly positive (eastward), while the meridional component was mainly negative
218 (southward). There were periods at Pulley Ridge with direction reversals, such as March to July
219 2014 and October 2014, with negative zonal component and positive meridional component. The
220 subtidal flow speed at this location showed a tendency to decrease throughout the period of
221 observations. There were pulses of up to 1 m s^{-1} from March 2013 to November 2013 that were
222 related to the Loop Current proximity to Pulley Ridge (Kourafalou et al., 2018). Flows at
223 Southern Dry Tortugas (SD in Fig. 2) were similar to those at Pulley Ridge only at a few
224 instances such as between March and July 2014 and in early May 2015. In general, Southern Dry
225 Tortugas current distribution was more similar to Northern Dry Tortugas (ND in Fig. 2) than to
226 Pulley Ridge, most notably in the meridional (north) component and during 2013 and early 2014.
227 This cursory inspection of the low-pass filtered velocities leaves unanswered questions on how
228 the flow structure was related from station to station. Analysis with the EOFs sheds light onto the
229 interrelationship among sites and their response to distinct forcings.

230

231 **4.2 EOF Analysis**

232 Results from EOFs indicated that subtidal unidirectional flow, as portrayed by modes 1
233 and 2 together, explained 87% of the variance. Eigenvectors provided the horizontal and vertical
234 structure of the flow fields (Fig. 3). Mode 1 showed that the flow direction at the 3 sites ranges
235 inside the same quadrant, even within 30°. At each location, the flow veered clockwise with
236 depth <20° but maintained the same general direction. The structure of Mode 1, which explained
237 63% of the variance of the flow may suggest interconnectivity among all sites, except where the
238 flow was nearly parallel (between Southern and Northern Dry Tortuga). Connectivity from
239 Southern Dry Tortugas to Pulley Ridge may have occurred when Mode 1 coefficients were
240 negative. The same could be said about connectivity from Northern Dry Tortugas to Pulley
241 Ridge. In fact, a reconstruction of Mode 1 showed very similar flow at the 3 sites after December
242 2013 (Fig. 4a). At the beginning of the time series, Mode 1 was similar at Pulley Ridge and
243 Southern Dry Tortugas, although weaker at the latter. In general, Mode 1 flows were strongest at
244 Pulley Ridge (both components). Eigenvectors of Mode 1 reveal a stronger connectivity between
245 the two reefs near the shelf-break (subject to oceanic current influence) than connectivity of
246 either shelf-break site with a location on the shelf interior. The site on the shelf is primarily
247 influenced by shelf currents.

248 Eigenvectors for Mode 2 showed flows with the same sign in the zonal component at
249 Northern and Southern Dry Tortugas (Fig. 3). The flow structure appeared divergent for positive
250 instances of the EOF coefficients but illustrated possible connections from Southern Dry
251 Tortugas to Pulley Ridge and from Northern Dry Tortugas to Pulley Ridge with negative EOF
252 coefficients. At the 3 sites, Mode 2 showed very little veering with depth, i.e., smaller (<15°)
253 direction change than Mode 1. However, Mode 2 eigenvectors at the Dry Tortugas sites had
254 larger vertical shears, i.e., larger differences in surface minus bottom speeds, than Mode 1
255 eigenvectors. The reconstructed Mode 2 (Fig. 4b) illustrated these concepts by displaying

256 practically no resemblance among sites. Southern Dry Tortugas exhibited the strongest flows
257 associated with this mode. The variability related to modes 1 and 2 was explored in detail with
258 wavelet transforms.

259

260 **4.3 Wavelet Transforms of EOF Subtidal Flows**

261 The wavelet transform of the time series of Mode 1 coefficients for the subtidal flow (Fig.
262 5a) showed monthly to seasonal variability (Fig. 5b). This is illustrated by the spectral energy of
263 Mode 1 being statistically significant at the 95% level (inside the thick contour of Fig. 5b) and
264 persistent throughout the observation period. The most energetic variability occurred at periods
265 of around 40, 90, and 120 days (Fig. 5b). Tidal fortnightly (13.6 and 14.7 days), as well as tidal
266 monthly (27.6 and 29.5 days), periodicities were influential in the Mode 1 signal. Synoptic
267 variability of 10 days was sporadic and of lesser energy than the variability with periods greater
268 than one fortnight. Synoptic variability was greatest in 2013 and decreased toward 2015, as
269 indicated by the downward sloping contour of 95% statistical significance (Fig. 5b). For Mode 2
270 (Fig. 6a), the wavelet power spectrum showed similar variability as Mode 1 in terms of dominant
271 periodicities. There were persistent energetic variations at periods >120 days (Fig. 6b).
272 Prominent periodicities also occurred at around 40 days in the autumn of 2014 and at near 60
273 days in late-summer of 2013 and 2014. As with Mode 1, synoptic variability of Mode 2
274 decreased from 2013 to 2015. Modes 1 and 2 of subtidal flows showed their greatest variability
275 (largest wavelet spectral amplitude) at periods greater than 1 month.

276

277 **4.4 Loop Current - Florida Current System**

278 The data set of sea surface height anomalies (SSHA) was also analyzed with EOFs to try
279 to identify an effective Loop Current index. In turn, the index could serve to link the variability

280 to the currents in the Pulley Ridge area. Results of the EOF analysis on the SSHA for the same
281 observational ADCP period (27 months) are shown in Fig. 7. Eigenvectors are portrayed in maps
282 of sea surface height in the Gulf of Mexico. Mode 1 describes a sea-surface bulge in the gulf's
283 central part, flanked by two depressions to the east and west. This spatial structure is related to
284 the positive coefficients of Mode 1 that occurred after February 2014 (Fig. 7). During the first
285 year of measurements, the subtidal currents exceeded 0.5 m s^{-1} at the Pulley Ridge region as they
286 flowed southeastward (Figs. 2 and 4a). Prior to February 2014, Mode 1 coefficients were
287 negative (Fig. 7) so the bulges on the Mode 1 map had opposite signs. Mode 1 explained only
288 ~21% of the variability of sea levels in the region so, by itself, it is not representative of an index
289 for Loop Current activity. Mode 2 explained almost as much variability as Mode 1 (~18%),
290 while its horizontal structure shows a short-amplitude Loop Current meandering around
291 northwestern Cuba (Fig. 7). Mode 2 also showed a sea level bulge toward the northern gulf,
292 south of the Mississippi Delta. The coefficients of Mode 2 displayed a clear annual cycle with
293 peaks in October and troughs in March-April. Mode 3 and Mode 4 displayed more bulges and
294 troughs than modes 1 and 2. Their temporal variability maintained their sign for longer periods
295 than the other two modes. Despite the signal deconstruction, it is challenging to derive a Loop
296 Current index that relates to the flow variability at the Pulley Ridge region.

297 Alternative indicators were explored further with the AVISO SSHA data. Sea level at the
298 typical Loop Current location (average in the northwestern square of maps on Fig. 7) could be
299 used as a proxy for Loop Current activity. This signal (Fig. 8a) was similar to an index
300 implemented in Kourafalou et al. (2018), which was based on water temperature fields. Both
301 Loop Current indicators had similar variability in 2014 and 2015 (Fig. 8a) but diverged in 2013.
302 The index based on water level had long-term variations that emulated, at least qualitatively,
303 Mode 1 subtidal currents at Pulley Ridge (Fig. 8a).

304 Another indicator of Loop Current activity was sought with AVISO sea level values just
305 to the northwest (NW) of Cuba. An index was determined from mean values in the southeastern
306 square of maps of Figure 7, a usual area of Florida Current evolution. It could also be regarded as
307 a ‘young’ Loop Current position. This water level signal off NW Cuba, still inside the Gulf of
308 Mexico, had remarkably similar variations to the normalized Florida Current transport (Fig. 8b).
309 Variations at shorter periods were disparate, relative to Mode 1 of subtidal currents.

310 Qualitatively, the Florida Current and the sea level off NW Cuba had an inverse
311 relationship to Mode 1 subtidal current variations at the Pulley Ridge region (Fig. 8b). The
312 qualitative relationships between currents at Pulley Ridge and Dry Tortugas (Mode 1) and
313 remote forcing indicate that, for the most part, when the Loop Current bulges up in the inner
314 Gulf of Mexico, sea levels drop off NW Cuba. Ultimately, this relationship could be the linkage
315 between ‘young’ and ‘extended’ phases of the Loop Current, which should be explored in the
316 future. Most evident is the result that subtidal currents in the Pulley Ridge-Dry Tortugas region
317 (Mode 1) respond inversely to water levels off northern Cuba, a precursor to the Florida Current.
318 Mode 1 of subtidal currents is compared to wind velocity components next.

319 **4.5 Wind Forcing**

320 Another potential driver of the subtidal variability in the flow around Pulley Ridge-Dry
321 Tortugas is wind. The wind components can be compared qualitatively to EOF modes 1 and 2 of
322 the subtidal flows (Fig. 9a). The eastward wind component was mostly negative throughout the
323 period of measurements, consistent with the influence of the Trade Winds, which blow westward
324 (Fig. 9b). There were sporadic eastward wind events, being most persistent in the period from
325 December 2013 to February 2014. These persistent eastward winds also had a southward
326 component associated with typical winter northwesterlies in the northern and eastern Gulf of
327 Mexico. The northward wind component displayed near-semiannual variations with southward

328 wind appearing mainly in the fall and winter (Fig. 9b). During the summer, this component was
329 positive but weaker than in the rest of the year as winds were dominated by the Trades influence.
330 Qualitatively, winds show no discernible relationship with modes 1 or 2 of subtidal currents (Fig.
331 9). In periods longer than one month, subtidal flows and winds overall seem to be disconnected.
332 At intra-monthly scales, there may be occasional relationship that requires further scrutiny. The
333 relationships between subtidal flows and Loop Current, as well as the linkage between subtidal
334 currents and wind forcing, are explored in the Discussion with wavelet coherence analysis.

335

336 **5. Discussion**

337 Subtidal flow variability in the Pulley Ridge area was related to Loop Current structure
338 and to wind forcing at different temporal scales, in agreement with numerical model results
339 (Kuorafalou et al., 2018). Quantitative linkages are explored in time, throughout the observation
340 period, and as a function of frequency (or period) of variability via comparison of the continuous
341 wavelet transform of each variable. Although the subtidal flow variability is highly
342 heterogeneous in space and time (Figs. 3 to 8), wavelet coherence analysis identified portions of
343 the record when variables were related and at what periods of variability. Figures 3 to 8 suggest
344 that there was no persistent response of the flow at Pulley Ridge to forcing from Loop Current or
345 wind. However, there were periods of clear Loop Current influence when approaching the Pulley
346 Ridge area, as in several months at the end of 2013. Some generalities could be drawn from the
347 wavelet coherence analyses described next.

348 Values of wavelet coherence between Loop Current index (black line in Fig. 8a) and
349 Mode 1 of subtidal current wavelets (Fig. 10a) were statistically insignificant most of the time.
350 Only at the beginning of the observation period there was a direct relationship between the two,
351 at fluctuations near one month. Other significant values appeared intermittently at periods

352 between 20 and 60 days (Fig. 10a). These are the portions on the diagram that are encircled by a
353 black contour and that show vectors. However, these apparent relationships had changing phases
354 (arrows changing directions) that made no physical sense (Grinsted et al., 2004).

355 In contrast to the Loop Current index-Mode 1 relationship, the wavelet coherence
356 between water level off NW Cuba (Fig. 8b) and Mode 1 subtidal currents at Pulley Ridge (Fig.
357 10b) had ~5-month fluctuations that were strongly coherent throughout the observation period.
358 The coherence between these fluctuations appear as a red band limited by a black contour,
359 centered at around 150 days (Fig. 10b). Because the arrows in that band are pointing roughly to
360 the left, Mode 1 and water level off NW Cuba were in near antiphase at those periodicities.
361 Antiphase between the variables indicated that decreases in water level off NW Cuba were
362 associated with increases of southeastward flows at the Pulley Ridge-Dry Tortugas Region. A
363 similar response with significant coherence (>95% confidence limit) occurred in fluctuations
364 with periods of ~2 months, centered at ~64 days, after mid-2014. The first few months of the
365 records were also coherent at 60 to 90 days (Fig. 10b) albeit falling outside the cone of influence
366 (Torrence and Compo, 1998), meaning that the relationship was tentative at that time. Thus, part
367 of the variability of currents in Pulley Ridge-Dry Tortugas could be related to remote forcing
368 related to the Loop Current - Florida Current system, as a ~5-month fluctuation appeared at both
369 records throughout the period of observations. An enhanced version of a Loop Current index is
370 needed to improve the exploration of the relationship between Loop Current and currents at
371 Pulley Ridge. Because it is challenging to constrain the Loop Current in terms of its position, of
372 the value of its surface topography, of its water temperature or of its flow conditions, future
373 efforts shall attempt to determine linkages with flows near the Yucatan channel. Sea levels off
374 NW Cuba, which are dominated by a 'young' phase of the Loop Current may provide a
375 promising index of such linkage. The next step was to investigate wind forcing.

376 The coherence of wavelet power spectra between the two components of wind velocity
377 and subtidal currents Mode 1 (Fig. 11) displayed sporadic linkages at periods <1 month. The
378 zonal component of the wind (Fig. 11a) was coherent with subtidal currents practically
379 throughout the period of observations, albeit at different intra-monthly periodicities. However,
380 autumn and winter displayed the most significant coherence between these two variables. For
381 example, coherence squared between these two variables was statistically significant in late 2013
382 and early 2014 at periods between 8 and 20 days. Similar response was recorded in late 2014 and
383 early 2015. The phase lag between eastward wind and subtidal currents was 180° (arrows
384 pointing leftward). This antiphase indicated that westward winds caused eastward currents at
385 intra-monthly periodicities. Moreover, most of 2014 exhibited significant coherence at periods
386 between 2 and 6 months.

387 The meridional component of wind (Fig. 11b) had less persistent periods with statistically
388 significant coherence than the east component throughout the observation span. Variations <1
389 month were also most prevalent in winter and autumn, when southward winds were strongest.
390 However, phases were inconsistent from one coherent period to another. Only two periods, one
391 in early 2014 and one in the autumn of 2014 (Fig. 11b), were consistent in their 90° phase lags.
392 This indicated a quadrature relationship between northward winds and currents in which
393 maximum currents were reached at the end of a northward pulse. Although eastward winds seem
394 to have been more influential than northward winds in the subtidal flow records, it was evident
395 that intra-monthly variations of wind influenced the flow at those periods.

396 It was also apparent that subtidal currents over the southern West Florida Shelf result
397 from an interaction between remote (Loop Current) and local (wind) forcing that is more
398 complex than the description presented here. The analyses carried out with the subtidal flow
399 considered only EOF Mode 1, which explained 63% of the observed variability. This Mode

400 described depth-independent flows moving in roughly the same direction at the 3 sites sampled.
401 Therefore, the analyses disregarded part of the variability that is more heterogeneous. The spatial
402 structure of the flow in the area is likely to describe eddies and recirculations, which were not
403 well defined in the records and not discussed. However, these eddies were evident in Kourafalou
404 et al. (2018), when combining mooring data with model simulations and satellite observations.
405 Three moored records of current velocities, alone, were insufficient to decipher such complexity.
406 A study solely based on *in situ* observations will require a much denser coverage of
407 measurements that resolve shelf, shelf-slope exchange, and remote processes.

408

409 **6. Conclusion**

410 Current velocity profiles were recorded for ~2.5 years at 3 sites on the southern West
411 Florida Shelf. Records documented shelf flows in a gulf with mesophotic corals greatly
412 influenced by a looping western boundary current. Results described the complexity of the flows
413 at the transition zone between a western boundary current (regional branches of the Gulf Stream)
414 and the shelf. Analyses of the velocity profiles found that most of the variability was represented
415 by nearly depth-independent flows moving approximately in the same direction at the 3 sites
416 sampled (EOF Mode 1). These flows were likely driven by remote forcing via the Loop Current
417 in extended (gulf interior) and retracted (near NW Cuba) phases at sub-monthly periodicities (>1
418 month) and by local forcing (winds) at intra-monthly periodicities (<1 month). Flow variability
419 related to more complex spatial structures is likely linked to the nuanced morphologic changes in
420 the area where the Florida Current interacts with shelf currents. Flows moving in the same
421 direction at the three sites sampled (EOF Mode 1) indicated more robust connectivity between
422 Pulley Ridge and Southern Dry Tortugas than between Northern Dry Tortugas and either of the
423 other two sites. This reveals that connectivity was stronger between the two reefs near the shelf-

424 break (subject to oceanic current influence) than with a location on the shelf interior, which was

425 influenced primarily by shelf currents.

426

427 **Acknowledgments**

428 The study was funded by the National Oceanic and Atmospheric Administration (NOAA)
429 Center for Sponsored Coastal Ocean Research under award NA11NOS4780045 (Project Title:
430 “Connectivity of the Pulley Ridge – South Florida Coral Reef Ecosystem”). Villy Kourafalou
431 acknowledges additional support by the National Academy of Sciences, Engineering and
432 Medicine (Gulf Research Program UGOS #2000011056). Ryan Smith acknowledges partial
433 support from the Physical Oceanography Division at NOAA’s Atlantic Oceanographic and
434 Meteorological Laboratory (AOML). The Florida Current cable and section data are made freely
435 available on the NOAA/AOML web page (www.aoml.noaa.gov/phod/floridacurrent/) and are
436 funded by the NOAA Climate Program Office – Global Ocean Monitoring and Observing
437 Program.

438

439 **References**

- 440 Androulidakis, Y., Kourafalou, V., Özgökmen, T., Garcia - Pineda, O., Lund, B., Le Hénaff,
441 M., Hu, C., Haus, B.K., Novelli, G., Guigand, C. and Kang, H. (2018) Influence of river -
442 induced fronts on hydrocarbon transport: A multiplatform observational study. *Journal of*
443 *Geophysical Research: Oceans*, 123(5), pp.3259-3285.
- 444 Boicourt W. C., W. J. Wiseman Jr., Valle-A. Levinson and L. P. Atkinson (1998) Continental
445 shelf of the southeastern United States and the Gulf of Mexico: In the shadow of the
446 western boundary current. In: *The sea*, vol. 11 (A. R. Robinson and K. H. Brink, Eds.).
447 John Wiley, Hoboken, N. J., pp. 135-182.
- 448 Brokovich E, Einbinder S, Shashar N, Kiflawi M, Kark S (2008) Descending to the twilight-
449 zone: changes in coral reef fish assemblages along a depth gradient down to 65 m. *Mar*
450 *Ecol Prog Ser* 371:253–262.
- 451 Chang, Y.-L., & Oey, L.-Y. (2013). Loop Current growth and eddy shedding using models
452 and observations: Numerical process experiments and satellite altimetry data. *J. Phys.*
453 *Oceanogr.*, 43, 669–689. <https://doi.org/10.1175/JPO-D-12-0139.1>
- 454 Etter P.C. (1983) Heat and freshwater budgets in the Gulf of Mexico. *J. Phys. Oceanogr.*, 3,
455 2058-2069.
- 456 Grinsted, A., J.C. Moore, S. Jevrejeva (2004) Application of the cross-wavelet transform and
457 wavelet coherence to geophysical time series. *Nonl. Proc. Geophys* 11, 561-566.
- 458 Gordon, A (1967) Circulation of the Caribbean Sea. *Journal of Geophysical Research* 72
459 (24): 6207–6223.
- 460 Hoegh-Guldberg, H., P.J. Mumby, A.J. Hooten, R.S. Steneck, P. Greenfield, *et al.* (2007)
461 Coral reefs under rapid climate change and ocean acidification, *Science*, 318, 1737–1742.

462 Johns, W., T. Townsend, D. Fratantoni, W. Wilson (2002) On the Atlantic Inflow to the
463 Caribbean Sea. *Deep-Sea Research Part I: Oceanographic Research Papers* 49 (2): 211–
464 243.

465 Kahng, S.E., Garcia-Sais, J.R., Spalding, H.L. et al. (2010) Community ecology of
466 mesophotic coral reef ecosystems. *Coral Reefs* 29, 255–275.
467 <https://doi.org/10.1007/s00338-010-0593-6>

468 Kaihatu, J.M., R.A. Hanadler, G.O. Marmorino, L.K. Shay (1998) Empirical orthogonal
469 function analysis of ocean surface currents using complex and real-vector methods.
470 *Journal of Atmospheric and Ocean Technology*. 15, 927-941.

471 Kourafalou V., Androulidakis, Y.S., Kang, H., Smith, R.H., Valle-Levinson, A. (2018)
472 Physical connectivity between Pulley Ridge and Dry Tortugas coral reefs under the
473 influence of the Loop Current/Florida Current system. *Progress in Oceanography*, 165, 75-
474 99.

475 Leben, R.R. (2005). Altimeter-derived loop current metrics. *Circulation in the Gulf of*
476 *Mexico: Observations and Models*. In: Sturges, W., Lugo-Fernandez, A. (Eds.), *American*
477 *Geophysical Union*, pp. 181–201.

478 Lee, T.N., E. Johns, N. Melo, R.H. Smith, P. Ortner, and D. Smith (2006) On Florida
479 Bay hypersalinity and water exchange. *Bulletin of Marine Science* 79(2):301–327.

480 Lee, T.N., N. Melo, E. Johns, C. Kelble, R.H. Smith, and P. Ortner (2008) On water
481 renewal and salinity variability in the northeast subregion of Florida Bay. *Bulletin of*
482 *Marine Science* 82(1):83–105.

483 Lesser, M.P., M. Slattery, J.J. Leichter (2009) Ecology of mesophotic coral reefs. *J. Exper*
484 *Mar Biol Ecol* 375:1-8.

485 Sheinbaum, J. J., Candela, A., Badan, & J. Ochoa (2002) Flow structure and transport in the
486 Yucatan channel. *Geophysical Research Letters*, 29(3), 1040.
487 <https://doi.org/10.1029/2001GL013990>

488 Sous, D., Chevalier, C., Devenon, J.L., Blanchot, J. and Pagano, M. (2017) Circulation
489 patterns in a channel reef-lagoon system, Ouano lagoon, New Caledonia. *Estuarine,*
490 *Coastal and Shelf Science*, 196, 315-330.

491 Sponaugle, S., T.N. Lee, V.H. Kourafalou and D. Pinkard (2005). Florida Current frontal
492 eddies and the settlement of coral reef fishes. *Limnology and Oceanography*, 50: 1033-
493 1048.

494 Stabenau, E., and K. Kotun (2012) Salinity and Hydrology of Florida Bay: Status and Trends
495 1990–2009. National Park Service, Everglades National Park, South Florida Natural
496 Resources Center, Homestead, FL. Status and Trends Report. SFNRC Technical Series
497 2012:1. 39 pp

498 Thomson, R.E. and W. Emery (2014) *Data Analysis Methods in Physical Oceanography*, 3rd
499 Edition. Elsevier Science, 728 pp.

500 Torrence, C. and G.P. Compo (1998) A practical guide to wavelet analysis. *Bull. Amer.*
501 *Meteo. Soc.*, 79(1), 61-78.

502 Vaz, A.C., Paris, C.B., Olascoaga, M.J., Kourafalou, V.H., Kang, H. and Reed, J.K. (2016)
503 The perfect storm: match-mismatch of bio-physical events drives larval reef fish
504 connectivity between Pulley Ridge mesophotic reef and the Florida Keys. *Continental*
505 *Shelf Research*, 125, pp.136-146.

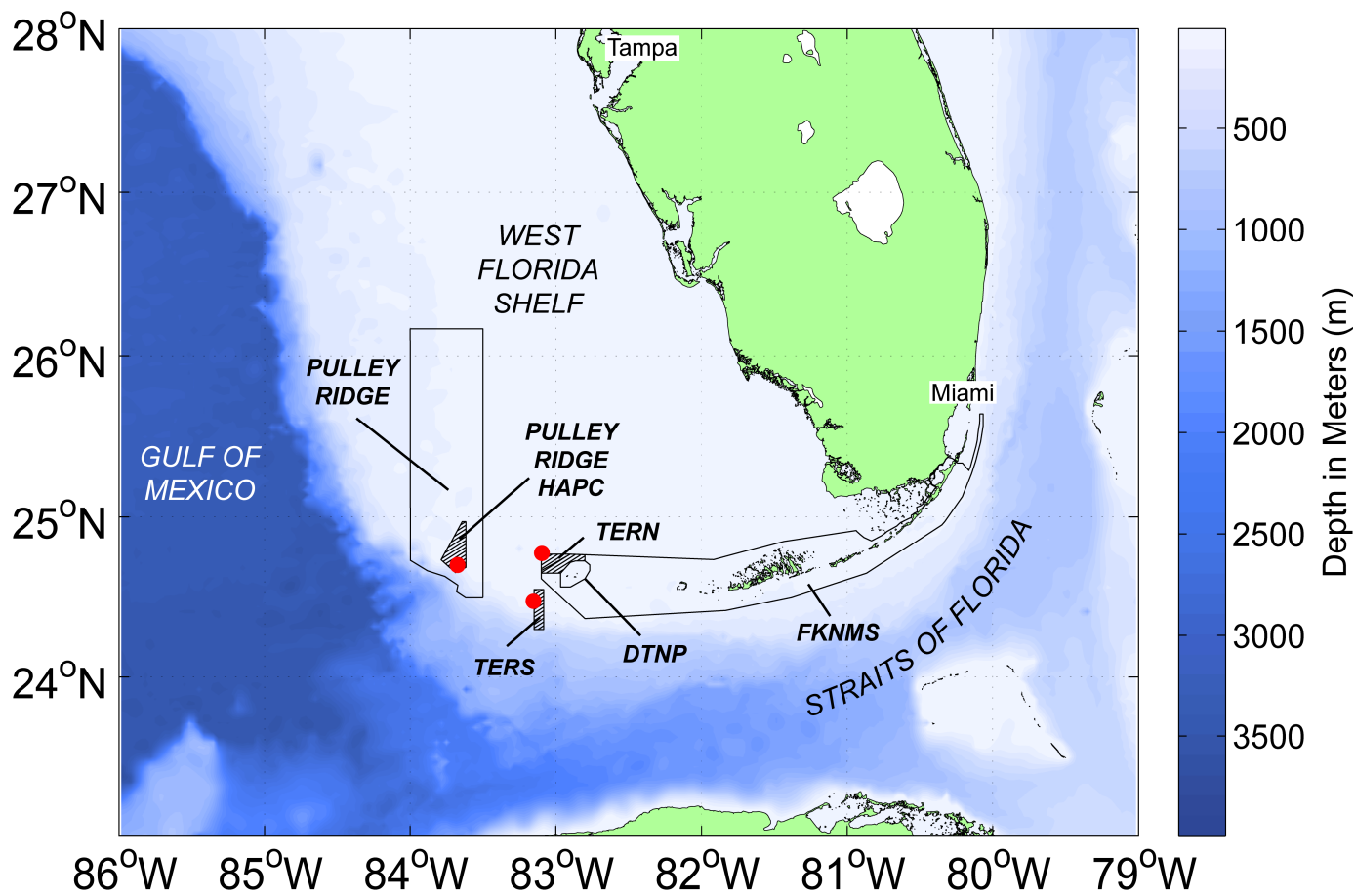
506 Weisberg, R.H. and Y. Liu (2017) On the Loop Current penetration into the Gulf of Mexico,
507 *J. Geophys Res, Oceans*, 122,12, 9679-9694, <https://doi.org/10.1002/2017JC013330>.

508 Zavala-Hidalgo, J., R. Romero-Centeno, A. Mateos-Jasso, S.L. Morey, B. Martinez-Lopez
509 (2014) The response of the Gulf of Mexico to wind and heat flux forcing: what has been
510 learned in recent years? *Atmosfera*, 27(3), 317-334.

511 Zlotnicki, Victor; Qu, Zheng; Willis, Joshua. 2016. JPL MEaSURES Gridded Sea Surface
512 Height Anomalies Version 1609. Ver. 1609. PO.DAAC, CA, USA. Dataset accessed
513 [2018-12-05] at <http://dx.doi.org/10.5067/SLREF-CDRV1>.

514

515

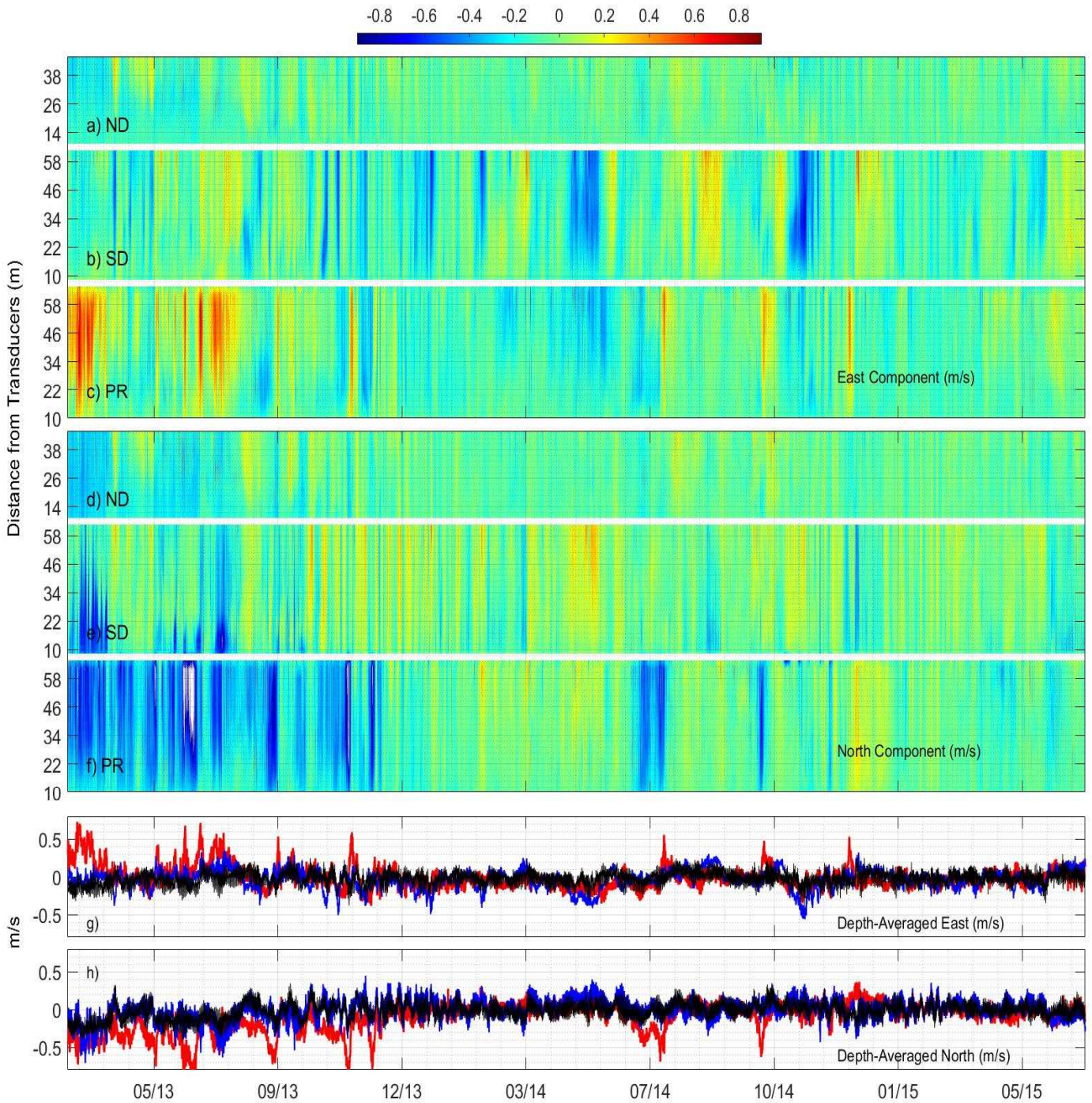


516
517

518 **Figure 1.** Study area in the eastern Gulf of Mexico, including the West Florida Shelf and Straits
 519 of Florida. Red markers represent moored ADCP locations at Pulley Ridge (Habitat Area of
 520 Particular Concern, HAPC), in the Northern Dry Tortugas (near Tortugas Ecological Reserve
 521 North, TERN), and in the Southern Dry Tortugas (near the Tortugas Ecological Reserve South,
 522 TERS). The boundaries of the Dry Tortugas National Park (DTNP) and the Florida Keys
 523 National Marine Sanctuary (FKNMS) are also shown for reference.

524

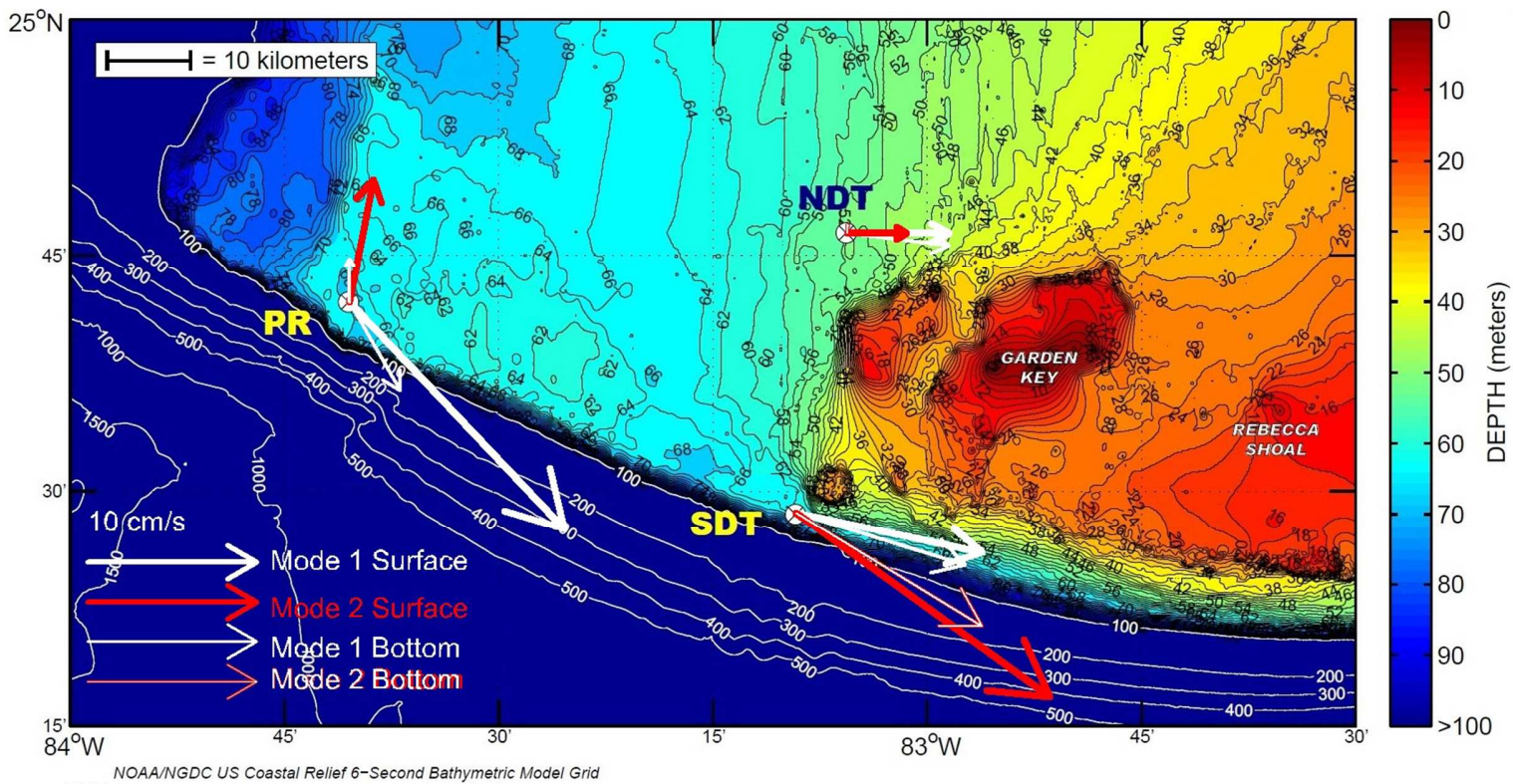
525



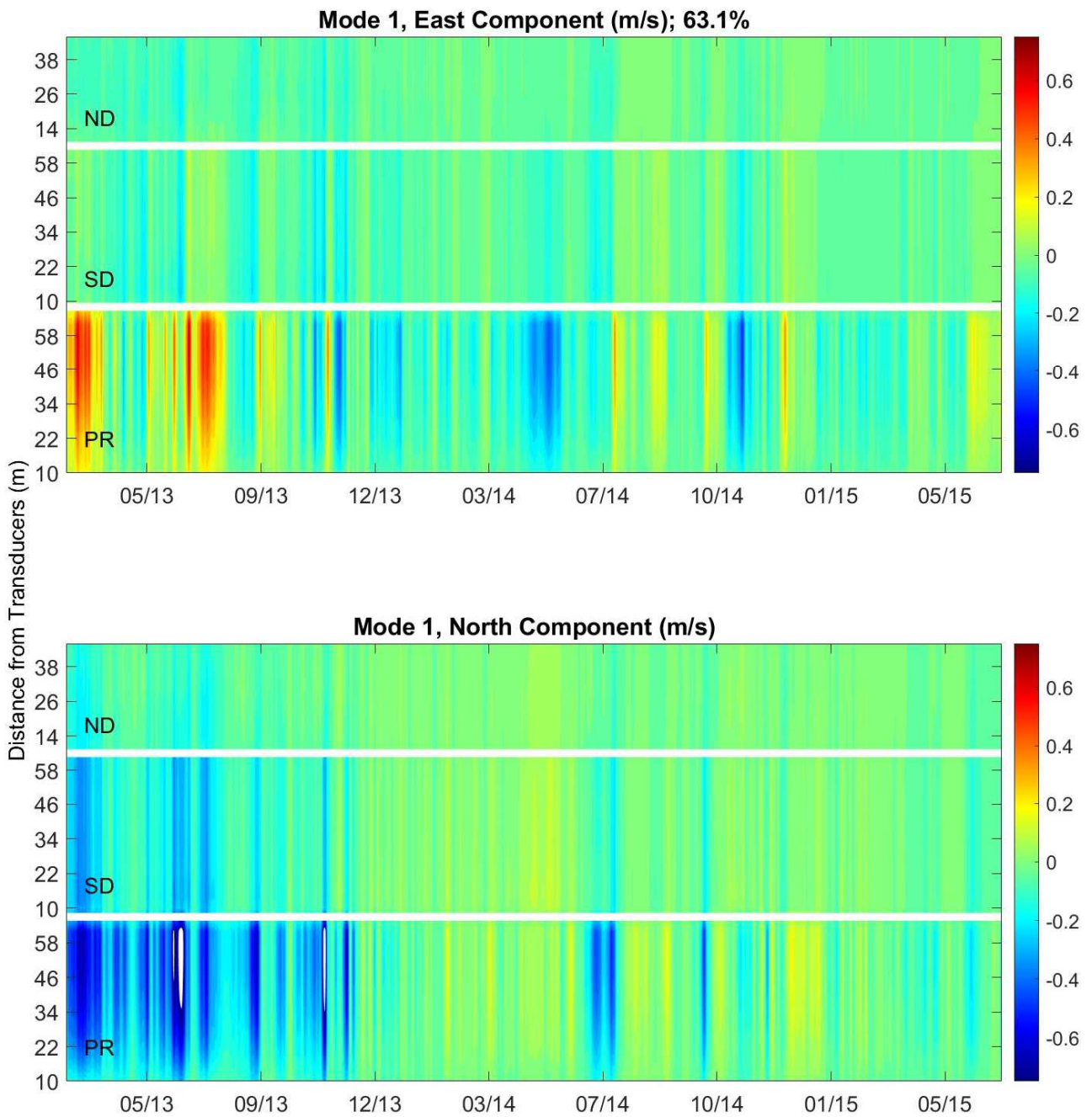
527 **Figure 2.** Low-pass filtered flow components (m s⁻¹) at the 3 sites during 27 months. a), b) and
 528 c) show the east component of the flow; d), e) and f) show the north component. PR is Pulley
 529 Ridge, SD is Southern Dry Tortugas, and ND is Northern Dry Tortugas. The vertical axis
 530 displays the approximate upward distance from the bottom at each one of the three sites. Positive

531 values (red) represent eastward and northward flow components. Panels g) and h) display the
532 corresponding depth-averaged values for PR in red, SD in blue and ND in black.

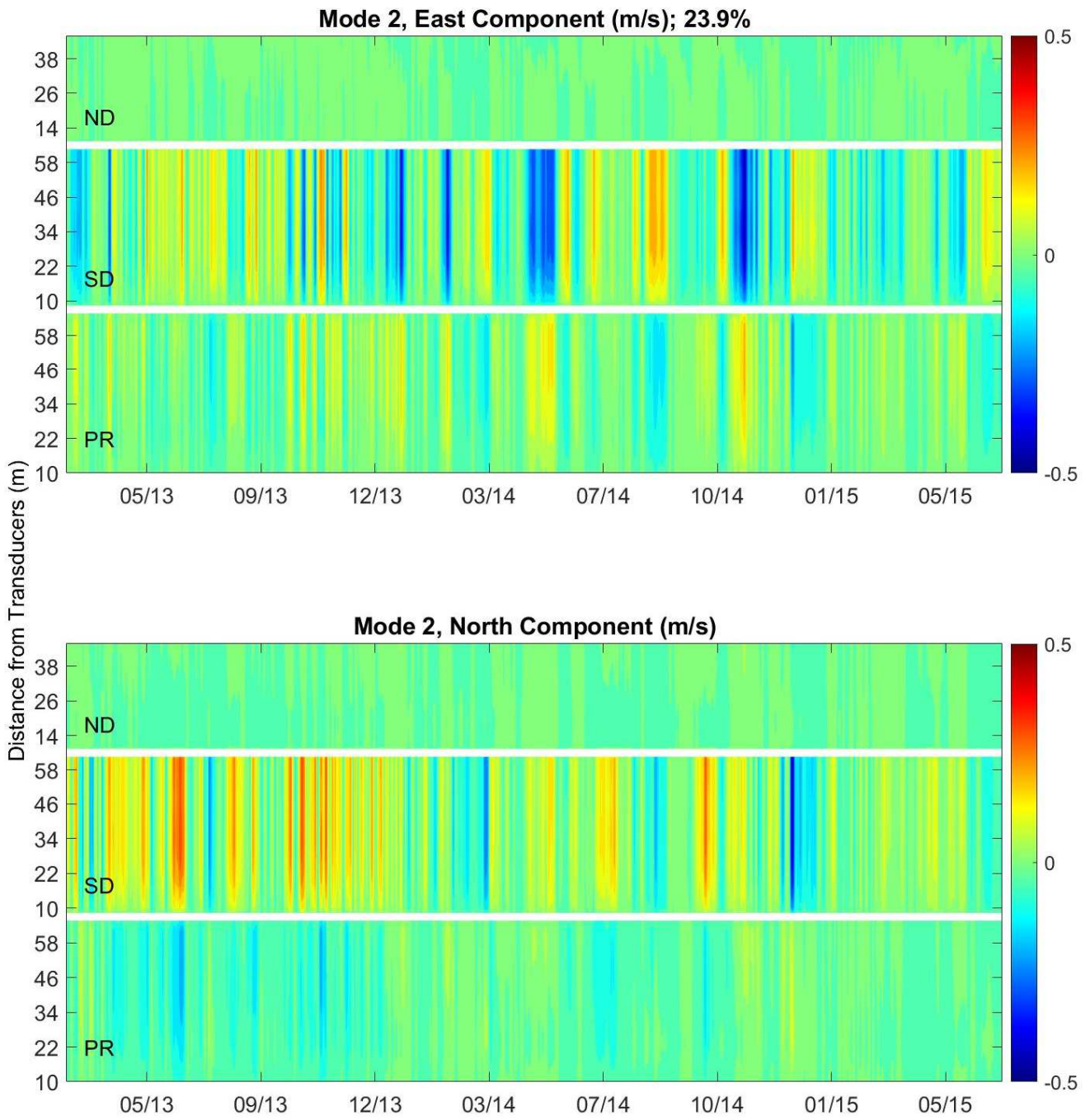
533
534



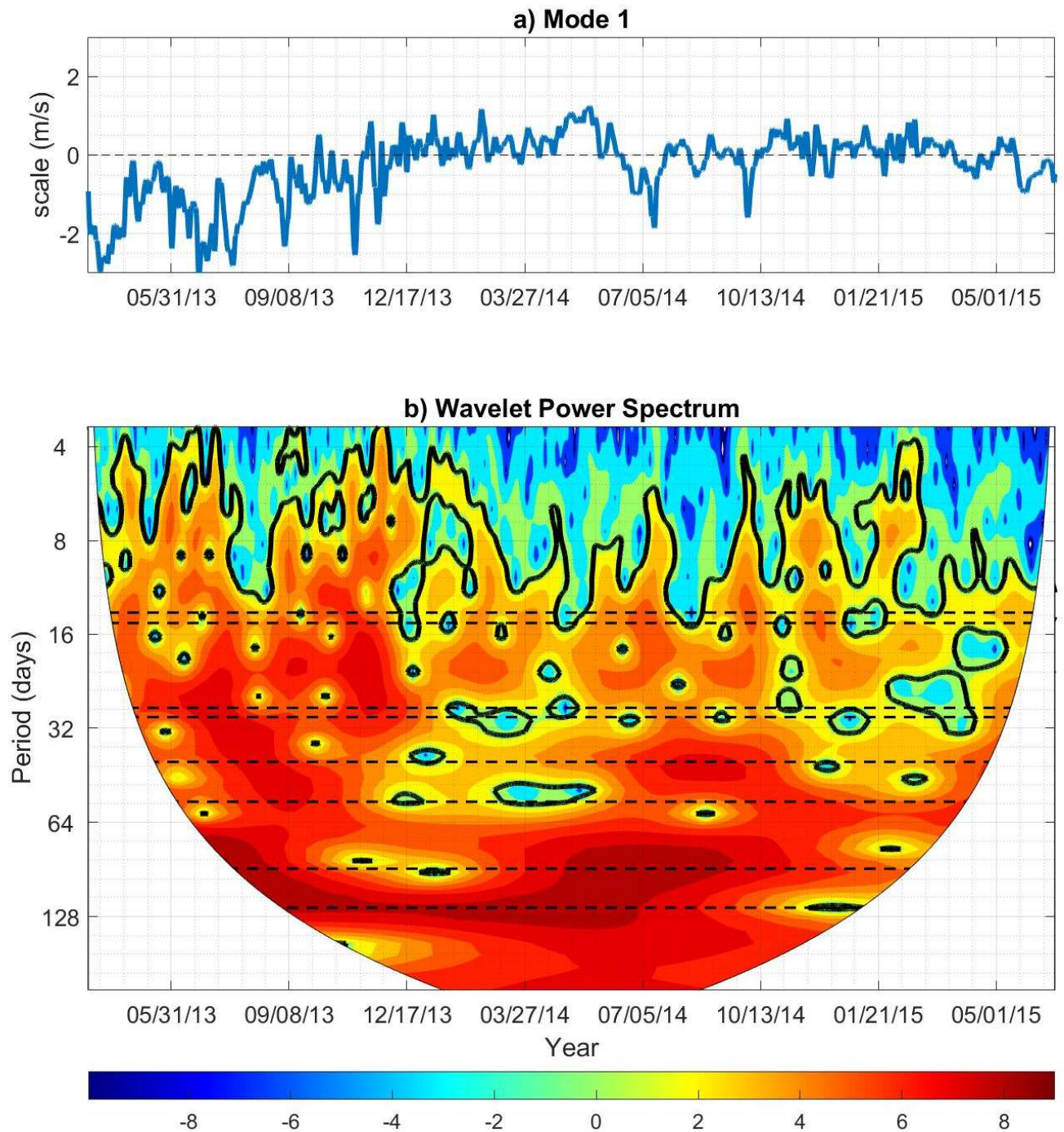
536 **Figure 3.** Vector EOF Modes 1 and 2 at surface and bottom. Pulley Ridge (PR), Northern Dry
537 Tortugas (NDT), Southern Dry Tortugas (SDT). Mode 1 explained 63.1% of the variability,
538 while Mode 2 explained 23.9%.
539
540



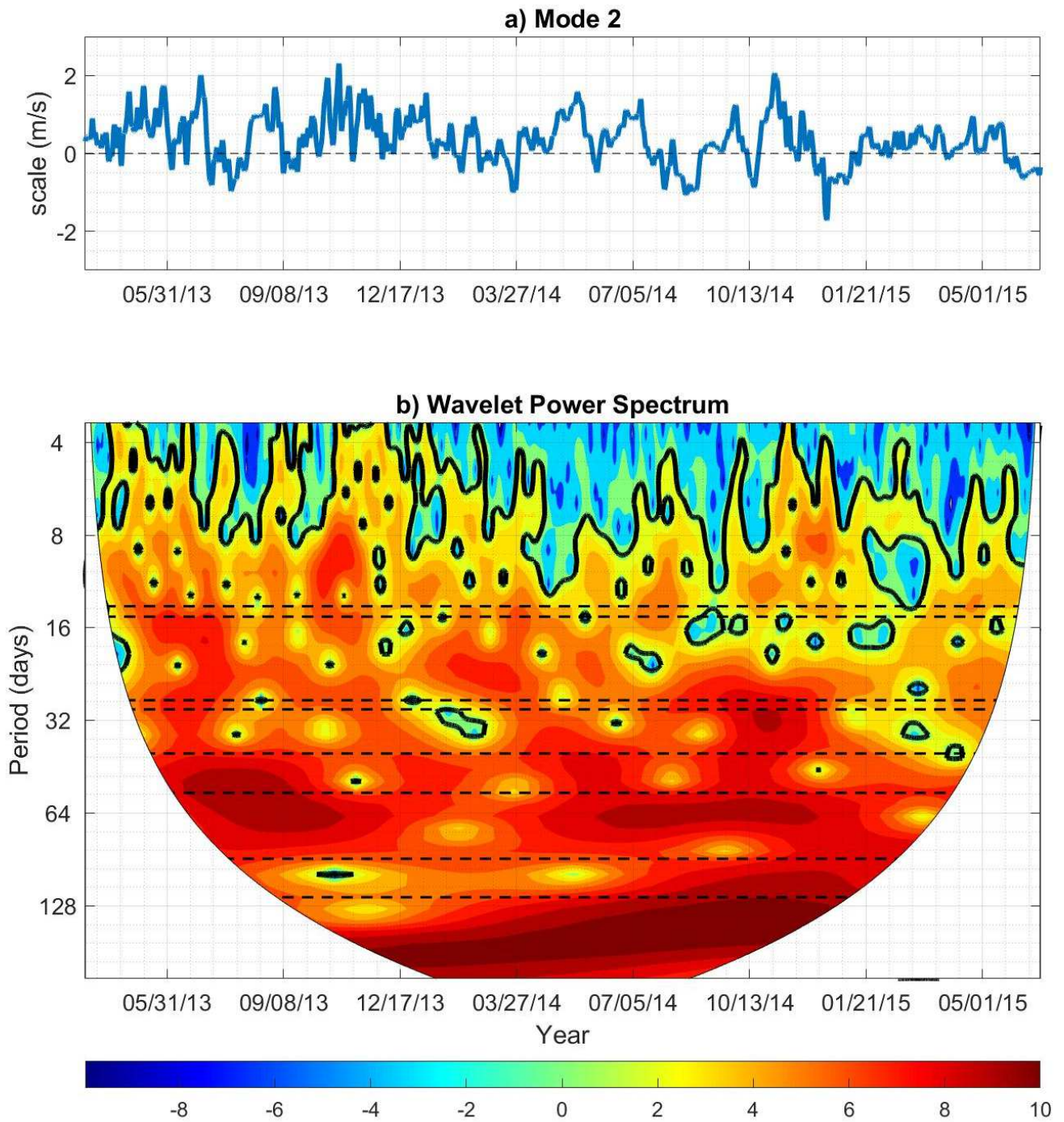
542 **Figure 4a.** Reconstructed EOF Mode 1. PR – Pulley Ridge; SD – Southern Dry Tortugas; ND –
 543 Northern Dry Tortugas. Explanation of figure is the same as Figure 2.
 544



546 **Figure 4b.** Same as Figure 4a, but reconstructed EOF Mode 2.
 547

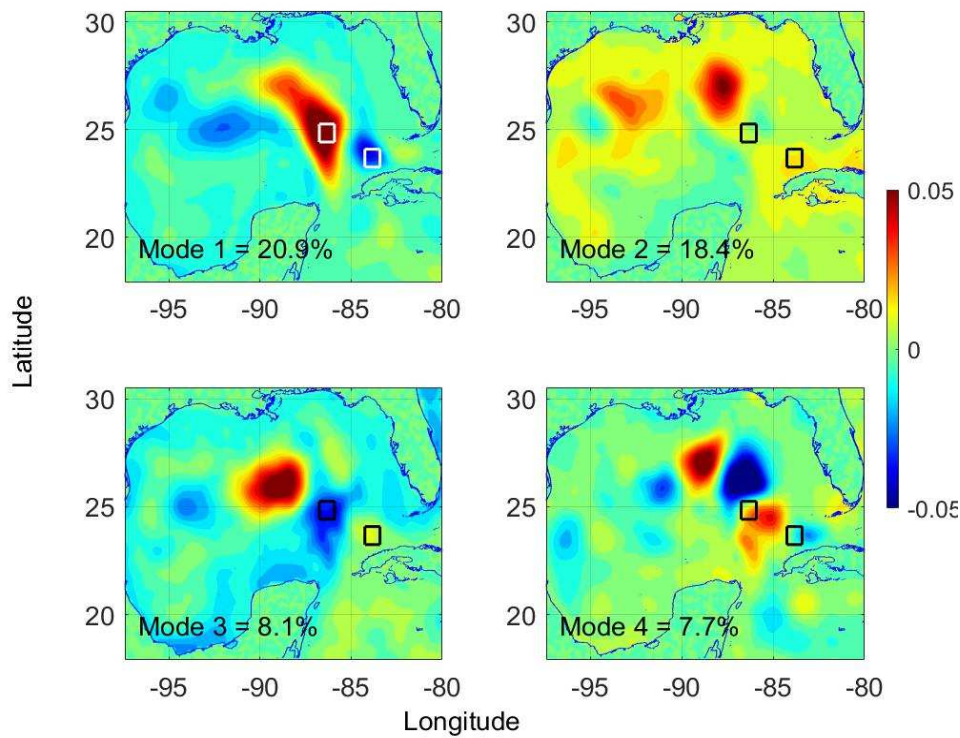


548
 549
 550 **Figure 5.** a) Scales or coefficients of Mode 1 shown in Figure 4a. b) Wavelet power spectrum
 551 (Morlet 4 wavelet) of EOF Mode 1 for subtidal currents. The 95% significance level is shown as
 552 a black contour. Horizontal dashed lines indicate periods, in days, of 13.7, 14.8, 27.6, 29.5, 41,
 553 55, 90, and 120.
 554

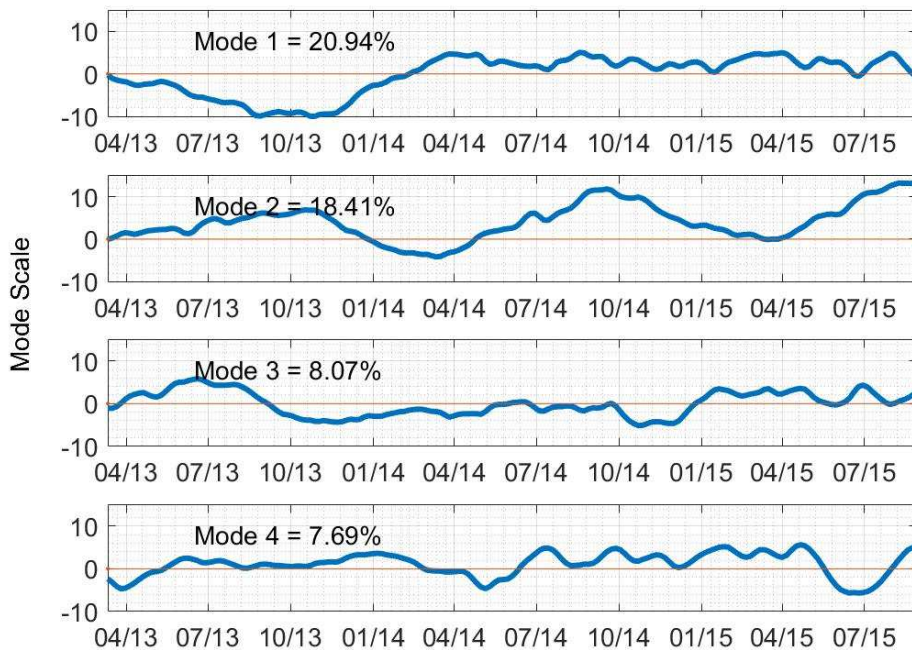


555
 556
 557
 558
 559

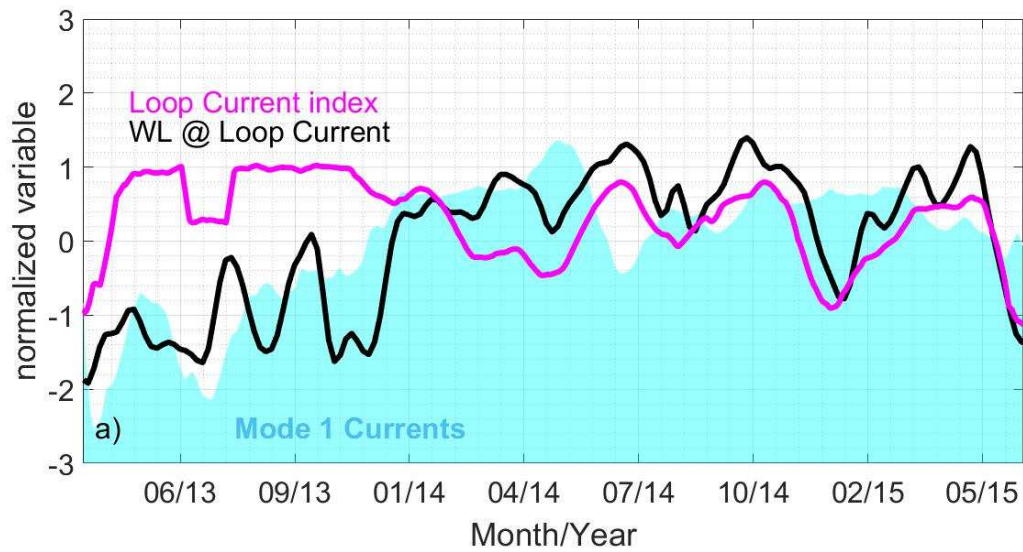
Figure 6. a) Scales or coefficients of Mode 1 shown in Figure 4b. b) Wavelet power spectrum (Morlet 4 wavelet) of Mode 2 for subtidal currents. Same as Figure 5.



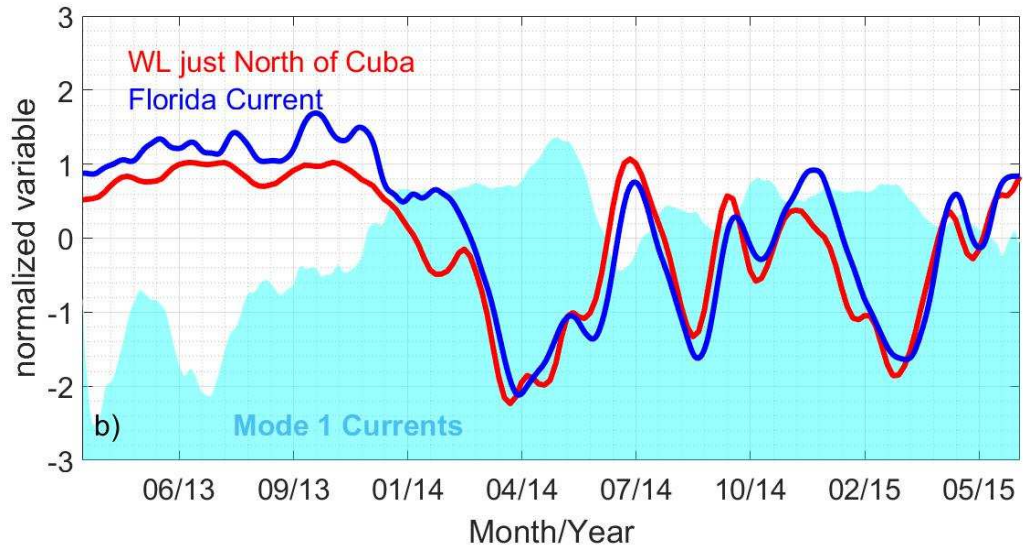
560
561



562 **Figure 7.** EOF analysis of SSHA for the period of ADCP observations. Shown on top are maps
 563 of first 4 eigenvectors and underneath are corresponding coefficients varying in time. Squares on
 564 maps indicate contrasting sites of water level variability shown in Figure 8.
 565



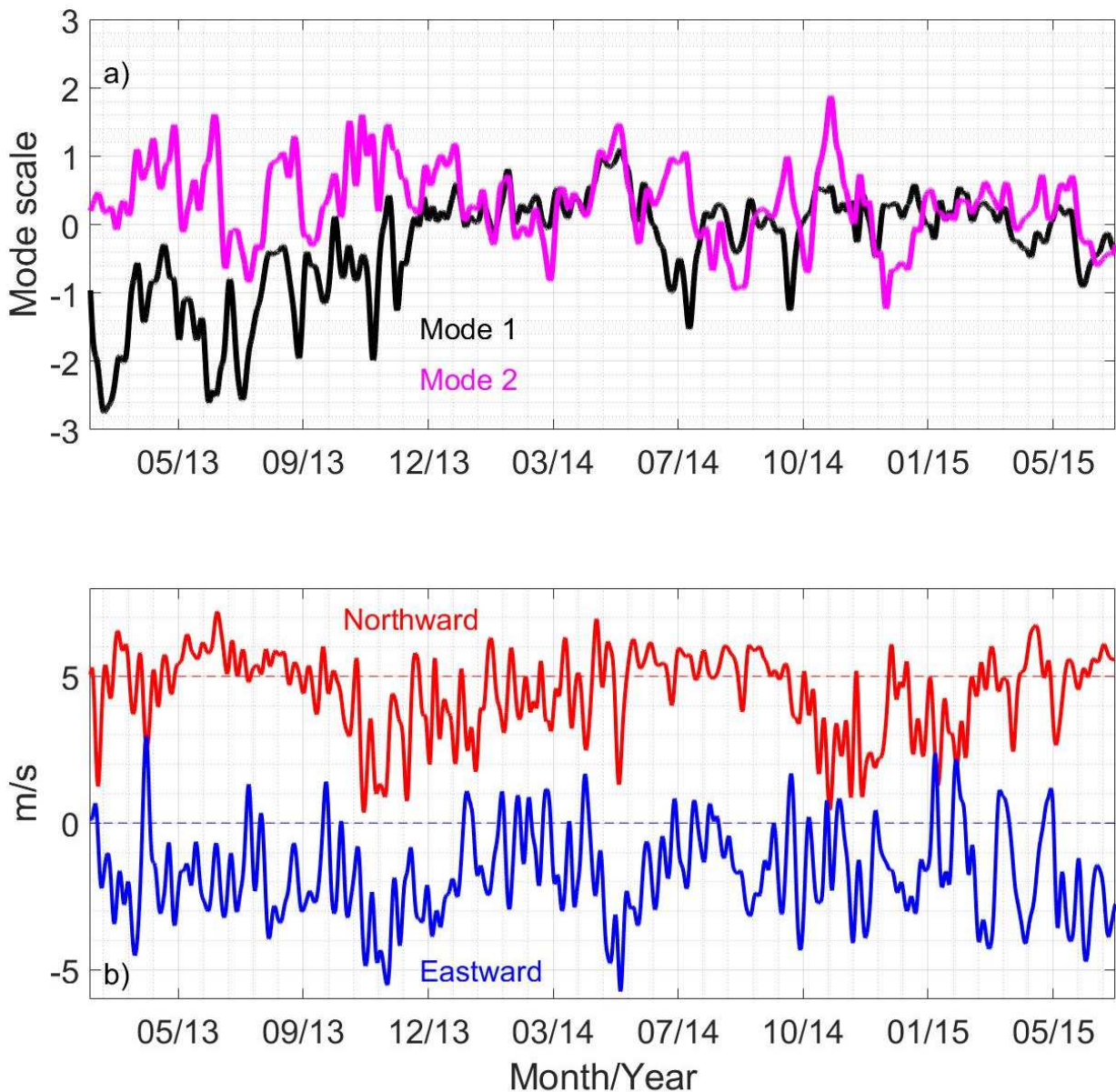
566



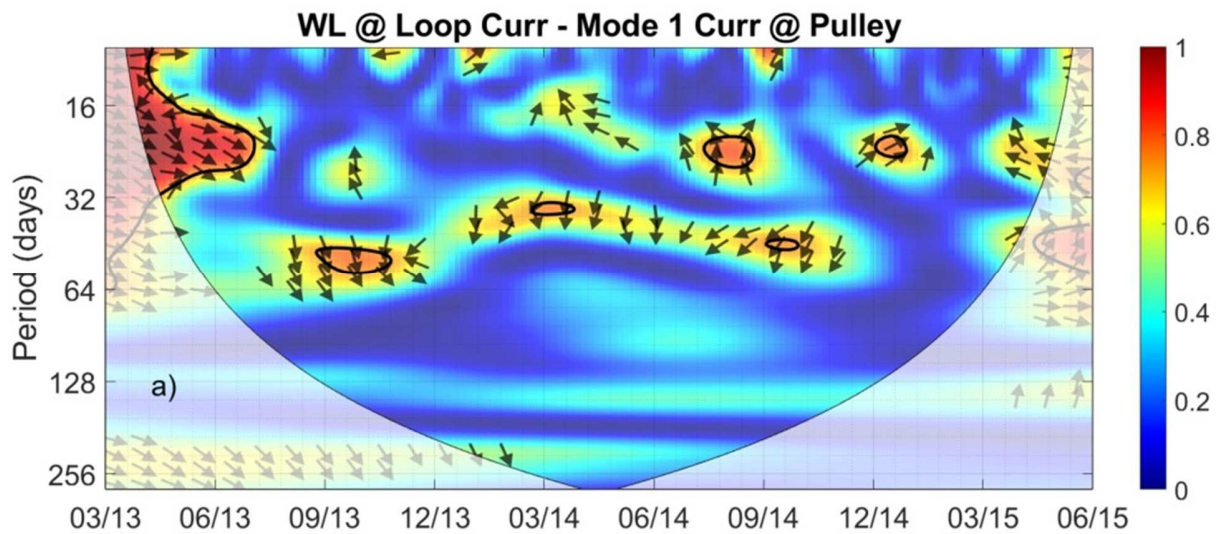
567

568

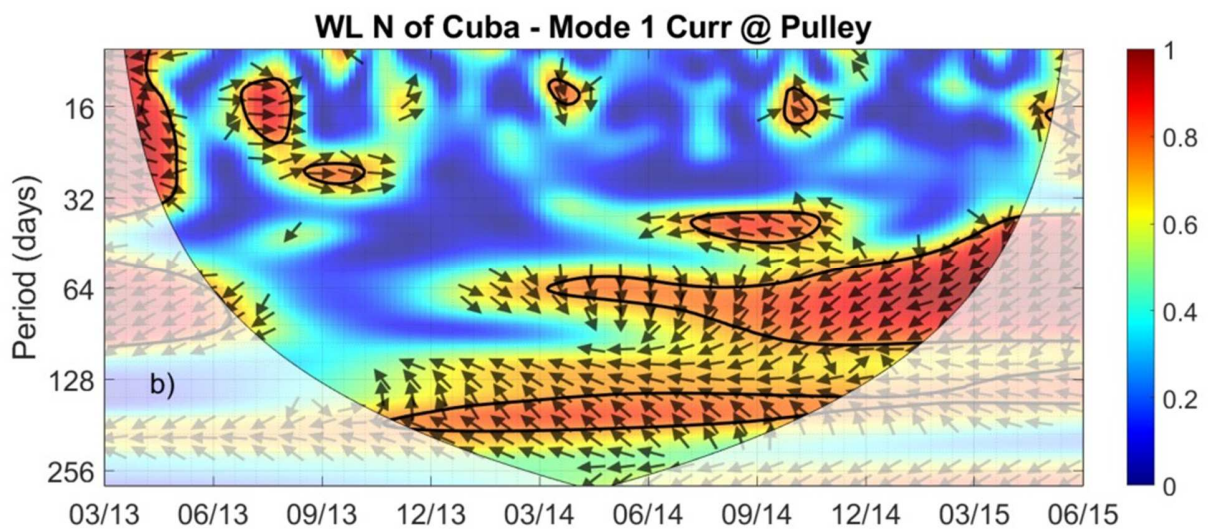
569 **Figure 8.** EOF Mode 1 for subtidal currents (shaded cyan signal) compared to Loop Current and
 570 Florida Current indices. a) The water level at Loop Current (WL @ Loop Current, black line) is
 571 the average at the northwestern square on the maps of Figure 7. The magenta line is derived from
 572 Kourafalou et al. (2018). b) The water level (WL) off the north coast of Cuba (red line) is the
 573 average of the southeastern square on the maps of Figure 7. All time series have been normalized
 574 by subtracting their mean and dividing by their standard deviation.
 575



577
 578 **Figure 9.** a) EOF Modes 1 and 2 for subtidal flows, and b) wind velocity components. All series
 579 have been filtered to 5 days. Wind velocity components are drawn in the oceanographic
 580 convention (direction toward which they blow). The Northward component has been displaced
 581 upward by 5 m s^{-1} to improve visualization.

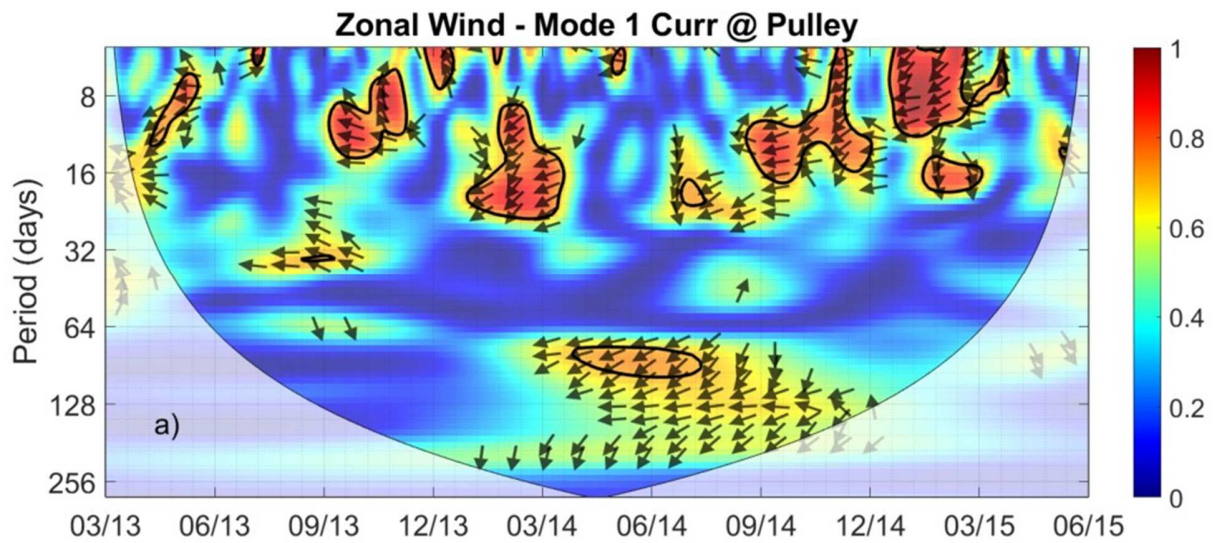


582
583

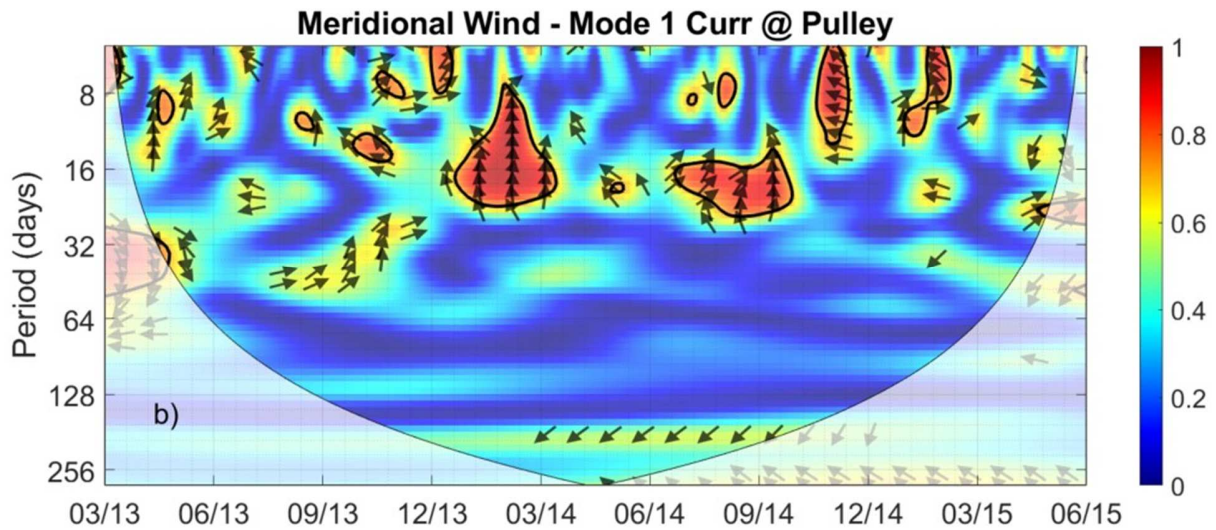


584
585

586 **Figure 10.** Wavelet coherence between a) Loop Current water level and Mode 1 for subtidal
587 currents at Pulley Ridge, and b) water level to the NW of Cuba and Mode 1 for subtidal
588 currents at Pulley Ridge. Thick black contour represents the 95% confidence level. Arrows denote phase
589 lag between the two variables. Arrows pointing to the right represent that the fluctuations of both
590 signals are in phase. Arrows pointing to the left indicate antiphase, and pointing upward describe
591 a phase lag of 90° . Translucent white regions feature the cone of influence.
592



593
594



595
596
597
598
599
600
601
602
603
604
605

Figure 11. Wavelet coherence between a) east component of wind velocity and subtidal currents Mode 1 at Pulley Ridge, and b) north component of wind velocity and subtidal currents Mode 1 at Pulley Ridge. Thick black contour represents the 95% confidence level. Arrows denote phase lag between the two variables. Arrows pointing to the right represent that the fluctuations of both signals are in phase. Arrows pointing to the left indicate antiphase, and pointing upward describe a phase lag of 90° . Translucent white regions feature the cone of influence.